Integrated Application of Remote Sensing and Spatial Statistical Models to the Identification of Soil Salinity: A Case Study from Garmsar Plain, Iran

Ali Akbar Noroozi,[1] Mehdi Homaee[*2] and Abbas Farshad[3]

1-PhD Graduate, Department of Soil Science, Faculty of Agriculture, Tarbiat Modares University, Tehran (Iran).

2-Professor, Department of Soil Science, Faculty of Agriculture, Tarbiat Modares University, Tehran (Iran).

3-Assistant Professor Department of Earth Science, Faculty of ITC, Twente University (Netherlands).

کاربرد تلفیقی سنجش از دور و مدل‌های آمار مکانی در شناسائی شوری خاک

علی اکبر نوروزی،¹ مهدی همایی*²، عباس فرشاد³

۱-دانش‌آموخته دکتری گروه خاکشناسی، دانشکده کشاورزی، دانشگاه تربیت مدرس

۲-استاد گروه خاکشناسی، دانشکده کشاورزی، دانشگاه تربیت مدرس

۳-استادیار گروه علوم زمین، دانشکده ITC، دانشگاه Twente هلند

چکیده

گسترش روند شورشدن خاک از چالش‌های مهم زیست‌محیطی عصر کنونی بـه ویژه در مناطق خشک و نیمه خشک است. به منظور شناسایی شوری خـاک، پژوهشی با تلفیق تصاویر ماهواره‌ای لندست TM در سال ۱۳۸۸ و مدل‌های آمار مکانی، انجام و تعداد ۲۸۸ نمونه در دشت گرمسار و ایوانکی از افق شناسائی سطحی خاک (میانگین ۱۵-۰ سانتی متر)، بـرای بررسـی ارتبـاط بـین هـدایت الکتریکی و بازتاب های طیفی ماهواره، برداشت و به آزمایشگاه ارسال شد؛ آنگاه آنالیز چند متغیره و به ویژه رابطه همبستگی مجذور حداقل متوسط (OLS) برای بررسی رابطه خصوصیات طیفی ماهواره و هدایت الکتریکی خاک انجام گرفت. در این رابطه، باند هفت ماهواره با طول موج بلند و شاخص انتقال طیفی۳(رطوبت خاک) در مدل اول و باند یک ماهواره در طول موج مرئی آبی، همراه بـا مولفه اصلی دوم در مـدل دوم درسـطح ۹۹٪ اطمینـان، حـدود ۶۰٪ از تغییـرات هـدایت الکتریکی را پیش بینی و بر آورد نمودند. ارزیابی دقت دو مدل با انجام اعتبار سنجی بر روی ۵۲ نقطه در دشت ایوانکی با شرایط مشابه دشت گرمسار انجام گرفت؛ پـس از آن از آماره های متوسط مطلق خطا و مجذور متوسط خطا بمنظور ارزیابی کیفیت و میزان خطای دو مدل تخمینگر، با دقت ۰/۴۹ دسی زیمنس و ۴/۱ دسی زیمنس استفاده شد. بنابراین با نسبت پایین میـزان مجـذور متوسـط خطـا، بـر آورد هدایت الکتریکی برای تولید نقشه شوری خاک مناسب تشخیص داده شد؛ سپس ارزیابی آنالیز حساسیت بر روی عوامل موثر در دو مدل نشان داد که باند مرئی یک و باند هفت مادون قرمز میانی، به ترتیب بیش از ۳ و ۲/۵ برابر نسبت به مولفه های اصلی۲ و شاخص انتقال طیفی ۳ در بر آورد شوری خاک حساس اند، بنابراین در استفاده از آن باید نهایت دقت را بکار برد.

کلمـات کلیـدی: آنالیز حساسیت، دشت گرمسـار-ایوانکی، شـوری خـاک، ماهواره لندست TM و همبستگی مجذور حداقل متوسط (OLS).

Abstract

Soil salinity expansion is an environmental challenge particularly in arid and semi arid regions. In order to evaluate the progressing extent of soil salinity in relation with natural and human-induced conditions, a study was conducted using the Landsat TM imagery. The present study was conducted in the Garmsar area to the East of Tehran. A total of 288 soil samples were analyzed to determine the relationship between the spectral reflectance and Electrical Conductivity (EC), as salinity indicator. Multiple regression analysis and Ordinary Least Square regression (OLS) were used to examine the relationships between EC and derived spectral to generate several models. In the case of derived spectral, mid-infrared band (TM Band-7), visible band (Band-1), Tasseled cap3 (Wetness index) and PCA2 (Principal Component Analysis) were found to be most correlated with the observed EC values of the surface layer of the soil, at 99% confidence level. The accuracy of the prediction model was tested using a validation set of 52 soil samples in Eyyanekey plain, close to study area where the environmental circumstance consist of similar properties. RMSE and MAE were used to evaluate the performance of the map prediction quality. Results showed that the appropriate model could predict the soil salinity with precision of 4.1 and 0.49 dS m^{-1}, respectively. The predicted salinity ranged from 0dS/m to 110dS/m. Therefore, the EC estimations were suitable to generate soil salinity map. Sensitivity analysis was tested on applied parameters that showed Band-1 and Band-7 were 3 and 2 times more than sensitive rather than other parameters respectively. The results are promising and certainly useful for soil salinity prediction.

Keywords: Electrical Conductivity (EC), TM, Ordinary Least Square regression, Garmsar (Iran), Soil Salinity.

* Corresponding author. *E-mail Address*: mhomaee@modares.ac.ir

Introduction

Soil salinization is one of the most widespread land-degradation processes that substantially limits crop productivity, and thus the food security (Epstein *et al.*, 1980). Soil salinity refers to the surface or near-surface accumulation of salts expressed in Electrical Conductivity (EC) of a solution extracted from a water-saturated soil paste (Richards, 1954; Farshad, 2008; Homaee and Schmidhalter, 2008). The five salinity classes—non saline (EC=<2 dS m^{-1}) through strongly saline (EC> 16 dS m^{-1}) — originally introduced by USDA (1951) is often used in soil survey interpretations. A slightly saline soil (EC= 4-8 dS m^{-1}) will not be suitable to some crops, whereas higher levels of salinity (EC>16 dS m^{-1}) will seriously hamper plant growth. Saline soils are generally characterized by a pH < 8 and an exchangeable sodium percentage (ESP) of below 15 (USSLS. 1969). The salinization process can occur either naturally (known also as 'primary salinization') or is human-induced (also known as 'secondary salinization'). Primary salinization refers to the accumulation of salts through a natural process, for instance when the soil parent material is salt-bearing, or when saline groundwater is the agent. Secondary salinization, on the other hand, refers to human interventions, mainly due to management failures.

The reported 30 million ha of salt-affected soils in Iran, which accounts for 21 percent of the country's land area (Momeni, 2007; FAO. 2008) occur mainly in the center, Southwest and Southeast of the country. These regions, representing one quarter of the country's surface area, have very low productivity compared to the rest of the country. The climatic conditions and their geopedological (geomorphology, lithology, hydrologic condition and soil) setting are the major causes of the widespread salinization (Pakparvar, 2004; Momeni, 2007; Abbassi, 2009). However, the role of human activities, such as, poor agricultural management practices, salt mining and construction of roads and reservoirs (Pakparvar, 2004) that lead to the secondary salinization remain an important issue. Mapping and monitoring is needed to generate temporal and reliable information on the nature, spatial extent, and temporal behavior of salt-affected soils in order to plan conservation and rehabilitation measures (Dwivedi *et al.,* 1997; Metternicht and Zink, 2003).

Soil Salinity Mapping and Monitoring

Salts (salinity) can occur in different sections of the soil profile; at the surface, near-surface or farther down in the subsoil. The occurrence of salts on the surface, mostly under low-rainfall and high-evaporation conditions, appears in various forms, such as white efflorescence, salt crusts, non-aggregated brown powder, black salt deposits and evaporative salt crystals.

Existing approaches to soil-salinity mapping and monitoring can be broadly put into two groups, namely 'proximate sense (ground-based)' and 'remote sensing based (air-born or space-born)' (Metternicht and Zink, 2009). The proximate approach includes field and laboratory methods, whereas the remote sensing-based approach includes use of aerial photographs and/or satellite data.

Remote sensing techniques have been used to map soil salinity directly from bare soil, and indirectly from vegetation in a real-time and

cost-effective way for large-area monitoring (Dwivedi *et al.,* 2001; Metternicht and Zink, 2003). The lack of vegetation or sparsely distributed vegetation on salt-affected soil surfaces makes it possible to detect the affected areas (Howari, 2003). A variety of remote sensing data has been used to identify and monitor salt-affected areas, including aerial photographs, video images, infrared thermography, visible and infrared multispectral, microwave images and hyperspectral imagery (Metternicht and Zink, 2009). Menenti *et al* (1986), Darvishsefat *et al.* (1999) and Alavi Panah and Zehtabian (2002) made use of Landsat Thematic Mapper (TM) bands 1 through 7 for identifying salt minerals (they found that Landat bands particularly SWIR bands has more strength to salinity detection). Saha *et al.* (1990) and Naseri (1998) recommend TM bands 3, 4, 5, and 7 for salt detection in Outarpradash in India and in the Gorgan plain in Iran, respectively. Madrigal *et al.*(2003) and Verma *et al.* (1994) detected soil salinity of cropped areas by correlating soil EC, determined at point sites within previously designated fields, to spectral values extracted from TM bands 2, 3 and 4, however, the integration of thermal band-6 led to solve the problem of spectral similarity in the latter case.

Rapid indirect techniques of inferring salinity, such as EC mapping are widely used as an alternative to laboratory measurements of soil solutions ions, which are time and resource demanding (Farshad, 2008).

It is repeatedly concluded that detection of soil degradation, particularly soil salinity, by conventional means of soil surveying is not only quite time demanding (Ghabour and Daels, 1993), but also quickly outdated, whereas remote sensing data and techniques offer the possibility for mapping and monitoring these processes more efficiently and economically (Shresta and Farshad, 2009). However, to assess the feasibility and the accuracy of satellite images to map and monitor salinity must be cross-checked with field measurements (Farshad, 2008). In this study, conducted in the Garmsar alluvial fan to the East of Tehran, remote sensing data and techniques are employed to determine the spatial extent and magnitude of salt-affected areas, whereas GIS-based facilities and modeling are used for the purpose of predicting the trend of salt movement in the soil.

Study Area and data

Garmsar is a city in Semnan Province, located about 82km Southeast of Tehran. It lies on an extensive alluvial fan at the edge of the Dasht-e Kavir, Iran's largest desert. The study area includes a part of the Garmsar alluvial fan and a smaller area in the Eyvanekey alluvial fan, which lies to the west of Garmsar, totally covering about 54000 km2. Elevation ranges from 161 to 244 m a.s.l. The climate is very dry (Aw according to the Köppen classification), with an annual rainfall of about 120 mm/year, which is negligible, as compared to the potential evapotranspiration (ET) of 1200 mm/year. The major water sources are the Hablerood (river) and a number of privately owned deep wells. The Hablerood, which flows through the area and finally into the salt lake in the Kavir (Fig. 1), plays also an important role in recharging the aquifers.
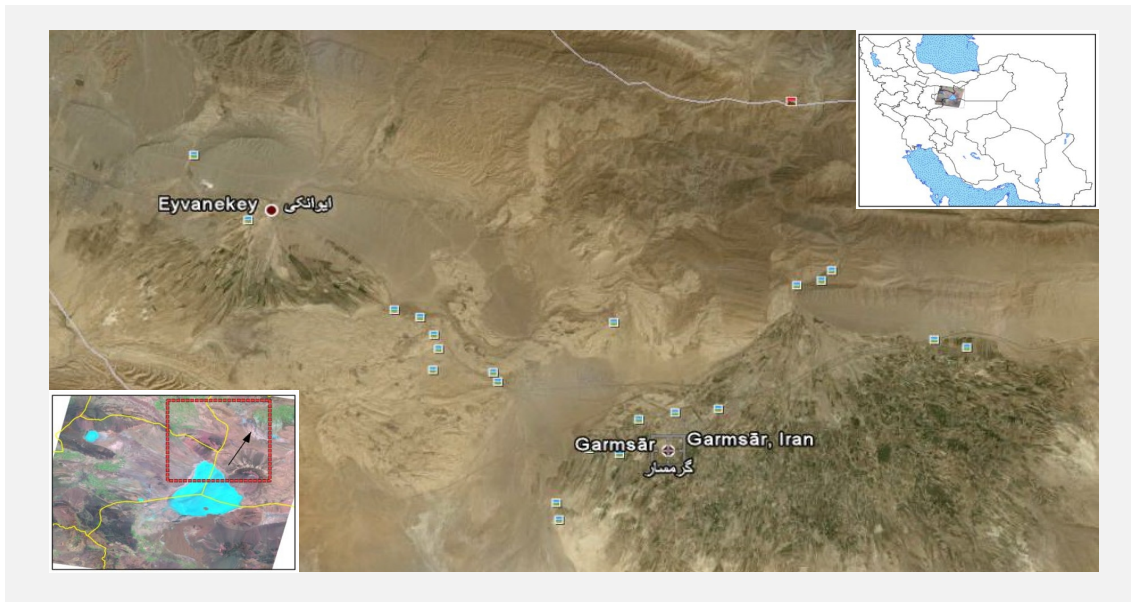
Figure 1. Location map depicting Garmsar and Eyvanekey (Source: Google Earth, Year 2009).

The fans and the glacis (Quaternary deposits) form the piedmont landscape, at the skirt of the heights, which stretch East to West in the North of the area, are composed of shale, gipsiferous marls, mudstone with sandstone and conglomerate, partly with gypsum rock formations. The lithological formations have led to mining salt (some 30 mines), sodium sulfate (14 mines), gypsum (6 mines) and many other minerals and rocks. It is reported that 70% of the salts and 30% of the sodium sulfate needed within the country is mined in Garmsar. Soils of the heights are dominantly Calcic Aquisalids and Typic Haplosalids, followed by Typic Torriortents along the lower slopes. The typical saline soils fall under Noreddin-Abad soil series (Pakparvar, 2004; Abbassi, 2009).

Due to its strategic position and the natural richness, Garmsar has had a long turbulent history. It was a disputed border town between the Medes and the Parthians (around 600 years

B.C.) and this was followed by many more disputed changes, to name only a few during the Sassanid (3rd through 6th centuries), the Samanid, the Ghaznavid, the Mongol, the Safavid and the Qajar periods. The settlers in the area are composed of some 20 tribal groups from different origins, such as Arab, Kurdish, Turkish, Lurrish, etc. Some tribal groups have preserved their pastoral and tribal methods of production. The Ossanlu, of Arab origin from Aman and Najd, are made up of several tribes and they chose cattle breeding once they arrived in the region, although they were occupied with cultivation before moving into the new area. The dairy and the meat produced by the nomads amount respectively to about 120 ton and 300 ton per year, traded in local markets. The issue of transhumant which is still practiced also plays an important role in soil degradation.

At present, both professions are exercised by the farmers. The dominant irrigated fields are

alfalfa, corn, wheat, barley in the uplands and sugar beet, cotton, and melon are major crops occupying the low lands. Beside some of the agricultural products such as wheat, barley, cotton, pomegranate, vegetables and melons, which are exported to some of the Persian Gulf States and to India, Ukraine, and a few African countries, salt, sodium sulfates and some other chemical substances, mined in the area, are also exported.

Materials and Methods

The foreseen research program, including this study, should ultimately lead to tracking down of salinization as a degradation process. The program comprises several GIS-oriented methods, next to the use of remotely sensed data and techniques, and the required fieldwork, that is an integrated approach to salinity mapping and prediction.

This paper is meant to cover the part that is allocated to the identification of soil salinity, wherein several investigations are applied; an integrated approach of remote sensing and spatial statistical modeling.

Soil Sampling

In total, 288 soil observations were made on a 1×1 km grid network, of which 236 in the Garmsar alluvial fan (Fig. 2) and the remaining 52 in the Eyvanekey fan, with similar physiographic conditions. The field survey was conducted in August 2009, approximately corresponding with the date of the remote sensing data acquisition. The coordinates of the observations were recorded using a Global Positioning System (GPS; Garmin etrex vista). The soil samples that were collected from the surface horizons (0-15 cm) were analyzed for a number of physical and chemical properties, of which EC plays a key role in this part of the study.
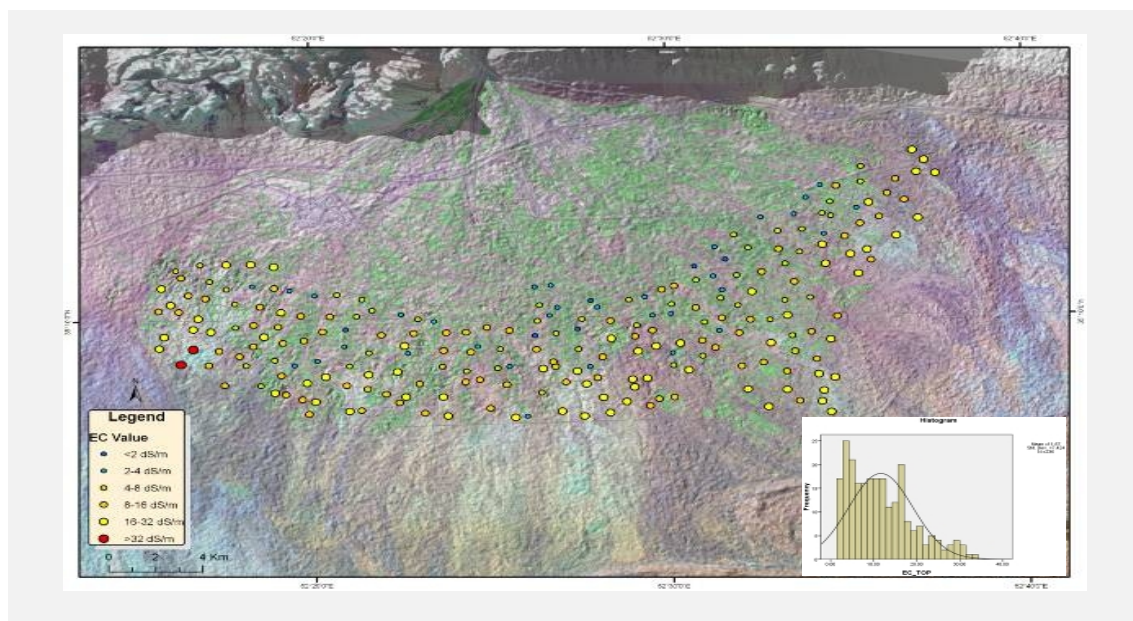

Figure 2. Distribution of the observation points in the Garmsar fan, Aug.2009.

In order to generate the topsoil salinity map, the mean of all EC-values within 0-15 cm depth, calculated for all the observation points, were used.

Extraction of Spectral Reflectance from Remote Sensing Data

The downloaded Landsat TM scene (Path 164 Row 36) of August, 11 2009 (*http://edcsns17. cr. usgs.gov/cgi-bin/EarthExplorer*), consisting of 7 bands with the ground resolutions (pixel size) of 30 m for the bands 1 through 5 and 7, and of 60 m for the band 6 was imported into ERDAS IMAGINE image processing software to generate a 'layer stack' for further treatments. The image was of good quality and no atmospheric corrections were performed. Geocoding, with an accuracy of less than one pixel (RMSE=0.87), was performed using topographic maps at a scale of 1/25000. Spectral values of the 7 original and 20 derived indices for corresponding observation sites were extracted making use of the "intersect values by point" command in ArcGIS (see the derived bands and the indices in Table 1).

Preparation of Spectral data

Besides the vegetation and salinity indices, Principal Component (PC) and Tasseled cap (brightness, greenness, wetness) indices were built in the "model builder" in ERDAS imagine in the graphical model (gmd) format. The derived images were overlaid by the image containing the soil sample sites. Pertaining spectral values were appended in the soil sample attribute table as "field column" (Table 1), making use of the "extract raster point value" command in ArcGIS.

Data Analysis

Twenty seven variables, consisting of 7 original bands, 3 PC and 6 tasseled cap transformations, 5 vegetation and 6 salinity indices were employed to examine their relationship with the EC values that were measured in the laboratory. The variables were selected according to their relative importance in the determination of salinity.

As the Pearson test (SPSS software, v.17) proved a high (at P<0.001) correlation, 'factor analysis', which is a multivariate technique for examining the underlying patterns or relationships between the variables (Hair *et al.*, 1992), it was applied to reduce the number of variables. Considering that variable independence is a requisite assumption, principal component analysis which reconstitutes the correlated "independent" variable and set them into a set of truly independent new variables (factors) was the next step. The analysis was performed using the orthogonal extraction method, which assumes that the extracted factors are statistically independent from each other. The first two components (Fig. 4) were selected on the basis of the cumulative variance percentage and an Eigen value of greater than one. A multiple regression analysis then helped to examine the relationship between the variables (in each of the two components) with higher correlation with EC, and higher-factor loadings. The technique that was followed to identify the significant predictor or independent variables was the stepwise forward estimation of sequential search. This process includes the predictor variables with higher partial correlation coefficients, in a sequential manner. This was separately examined

for all the components, in three groups (components) of respectively 11, 13 and 3 variables, including vegetation indices, tasseled cap 2 (greenness) and 3 (wetness), Landsat TM bands 6 and 7 and second component including Landsat TM bands 1 to 5, PCA 1 to 3, Tasseled cap 1 (Brightness) and salinity indices (SI1, SI2, SI3, NDSI, NDMI). The third component including the three tasseled cap images 4, 5 and 6 were left out of the analysis, as they form only 3% of the total variance.

Results

Analysis of the Variables yielded the mean value (M), standard deviation (SD) and correlation coefficient (r) of each variable with the observed EC (Table1).

Table 1. Descriptive data.

Variable	Description	Mean	Std. Deviation	Correlation with EC (r)
EC_TOP	Electrical Conductivity of Soil dS/m	11.674	7.424	100
SI1	Salinity Index 1 ($\sqrt{G \times R}$)	141.051	20.736	.596[**]
SI2	Salinity Index 2 ($\sqrt{G2+R2+NIR2}$)	156.878	24.335	.648[**]
SI3	Salinity Index 3 ($\sqrt{G2+R2}$)	114.865	27.025	.734[**]
NDSI	Normalized Differential Salinity Index (R-NIR/ R+NIR)	-0.076	0.128	.610[**]
BI	Brightness Index ($\sqrt{R2+NIR2}$)	141.051	20.736	.596[**]
NDVI	Normalized Differential Vegetation Index(NIR-R/ NIR+R)	0.076	0.128	-.610[**]
SAVI	Soil Adjusted Vegetation Index(NIR-R/ NIR+R+L)	0.114	0.191	-.610[**]
SATVI	Soil Adjusted Total Vegetation Index	-84.901	2.943	-.541[**]
MSAVI	Modified Soil Adjusted Vegetation Index	0.119	0.191	-.658[**]
EVI	Enhanced Vegetation Index	-0.190	0.301	.637[**]
NDMI	Normalized Differential Moisture Index	-0.143	0.093	-.549[**]
BAND1	Reflectance value of Band 1 (Blue visible)	114.818	20.692	.763[**]
BAND2	Reflectance value of Band 2 (Green visible)	68.309	14.549	.746[**]
BAND3	Reflectance value of Band 3 (Red Visible)	92.284	23.029	.725[**]
BAND4	Reflectance value of Band 4 (Near Infrared)	105.343	13.515	.183[**]
BAND5	Reflectance value of Band 5 (Middle Infrared)	142.076	26.714	.669[**]
BAND6	Reflectance value of Band 6 (Thermal)	170.284	5.822	.536[**]
BAND7	Reflectance value of Band 7 (Far Infrared)	79.767	20.180	.716[**]
PCA1	Principal Component 1	304.357	39.294	.735[**]
PCA2	Principal Component 2	0.995	15.744	-.648[**]
PCA3	Principal Component 3	1.624	18.655	-.647[**]
TAS1	TASSELED CAP1 (Brightness)	240.433	38.536	.703[**]
TAS2	TASSELED CAP2 (Greenness)	-24.409	21.498	-.705[**]
TAS3	TASSELED CAP3 (Wetness)	-29.963	11.977	-.549[**]
TAS4	TASSELED CAP4	43.764	6.165	.668[**]
TAS5	TASSELED CAP5	-18.295	6.680	-.473[**]
TAS6	TASSELED CAP6	-2.731	1.471	-.436[**]

**Significant at the 0.01 probability level

As shown in Table 1, the highest correlation with EC is for B1 (r .763) followed by B2 (.746), PCA1 (.735), SI3 (.734), B3 (.725), B7 (.716), Tasseled cap2 (-.705), Tasseled cap1 (.703), and the lowest value (.183) is for B4. The table also shows that the vegetation indices are negatively correlated with EC. Out of the 27 variables, with P < 001 for the entire set (Clifford *et al.*, 1989), three factors, with Eigen value of greater than one, could be extracted after examining the Scree plot (Fig. 3) under normalized Varimax rotation while carrying out factor analysis. The cumulative variance explained by the first two components was 81 percent with a cumulative variance of 42 percent for the first component and 39 percent for the second one. The variables under component 1 and 2 that showed higher factor loadings of > 0.7 were considered eligible for the regression analysis. Another group of variable, tasseled cap 4, 5, 6 under component 3, is omitted. Finally, the remaining 24 variables were selected based on either higher factor loadings and/or higher correlation with EC to include in the final regression analysis to examine the significant predictors of EC.

EC and Variables in component 1

Stepwise regression was run to examine the relationship between EC and the eleven predictor variables (two original Landsat bands 6, 7, five vegetation indices, and the four derived bands, namely Tasseled cap 2, 3, NDMI and NDSI). Following the regression estimates of fitting a multiple linear regression models (Hastie *et al.*, 2001), eight models were fitted in the regression. Model 2 (Band-7 and Tasseled cap3) turned out to have the best variation inflate factor (of less than 10), and the highest R2. A P-value of .000 indicates that there is a statistically significant (Draper and Smith, 1998) relationship between the selected variables at the 99 percent confidence level. The R^2 indicates that the model explains about 58 percent of the variability in EC. Although the variation explained by the model is moderate, but it demonstrates that the usefulness of the Landsat band 7 as compared to the other bands for detecting soil salinity. The standard error of the estimate (SE), which shows the Standard Deviation (SD) of the residuals, was 4.836. Furthermore, slightly high Durbin-Watson (DW) statistics (1.913) gives an indication of
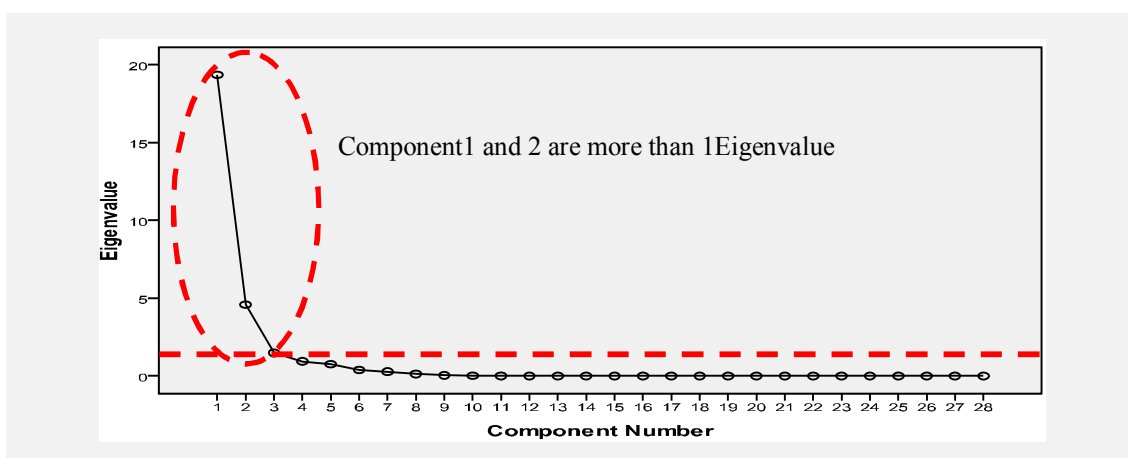

Figure 3. Scree plot.

some autocorrelation among the variables. Based on the selected model (formula1), an EC prediction map was drawn by GIS application and assorted in 5 standard EC classes (Fig. 4 left).

EC= -14.55+0.476*Band7+0.393Tasseled cap3   *(formula 1)*

EC and Variables in Component 2

In the same way, the stepwise regression was run this time with the 13 predictor variables (five original Landsat bands 1 through 5, Salinity indices -SI_1, SI_2, SI_3-, brightness index (BI), PCA 1, 2, 3, and Tasseled cap1). This time, Band1 and PCA2 were turned out to be statistically significant. The R^2 indicates that the model explains about 60 percent of the variability in EC and Standard Deviation (SD) of the residuals, at 4.72. Based on the selected model (formula 2), an EC prediction map was drawn by GIS application and assorted in 5 standard EC classes (Fig 4 right).

EC= -31.66+ 0.376*Band1+ 0.147*PCA2   *(formula2)*

Discussion

The EC variability explained by these models is 76 and 77 percent. Further statistical treatments show that: (1) there is no autocorrelation in the residuals; (2) both models and the contained variables are statistically significant at 99 percent confidence; (3) the negative intercept of the models is a indication of slight under-estimation; and (4) the Partial Correlation Confidence (PCC) indicates that Band 1 is very strongly correlated with EC as compared to the other bands, which were found to be only moderately correlated. The PCC measures the strength of the relationship between the dependent variable (EC) and each of the predictor variables, while the effect of the other predictor variables in the model is held constant. The adjusted coefficient of determination (Adjusted R2), which is useful for drawing a comparison between the models containing different numbers of predictor variables (Hair *et al.*, 1992), ranged from 0582 to 0598.
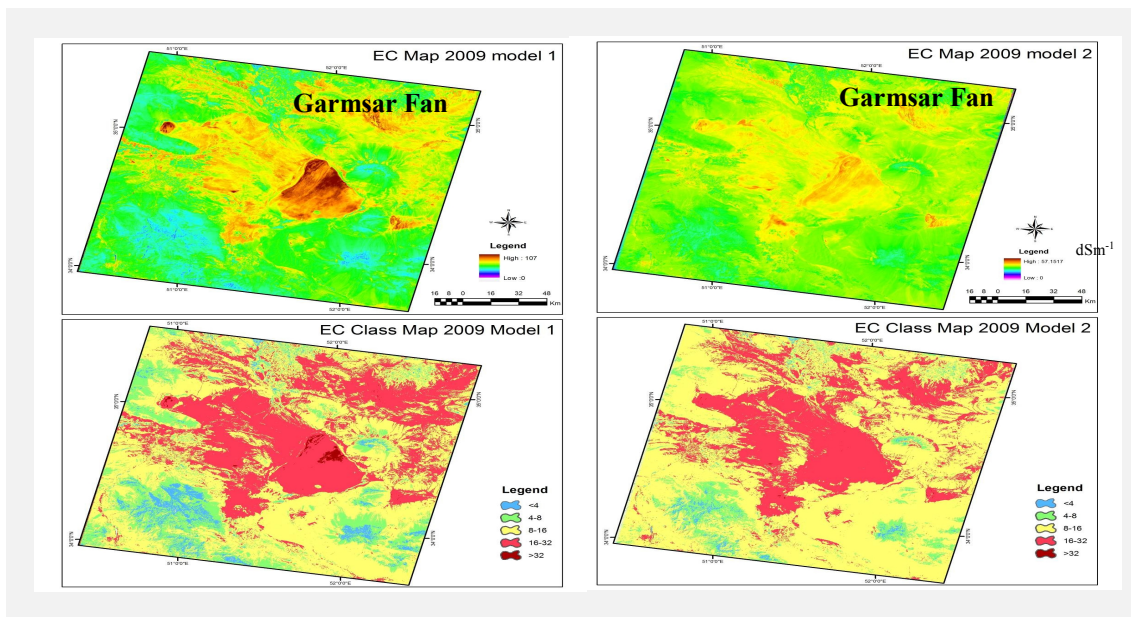

Figure 4. EC map extracted by Model 1 (left) and model 2 (right).

Higher coefficients indicate the relative superiority of the model containing a higher number of predictor variables, which may have little practical implication, if the range of explained variability is not wide. In order to confirm the applied statistical treatments and to select the appropriate model, the OLS (Ordinary Least Square Regression) tool in ArcGIS was adopted. This helps test the models for heteroskedasticity (inconsistence of residual variance) and non-stationarity (regional variation of independent variable) (Fotheringham *et al.*, 2002). OLS provides a global model of the variable or process and creates a single regression equation to represent that process (Table 4) (Andri Baltensweiler, 2010). The Koenker's studentized Bruesch-Pagan test indicated that our model violated the homoskedasticity assumption and it revealed non-stationarity. ArcGIS computes standard errors that are robust in regard to these problems. The robust probabilities were then consulted to determine the significance of the explanatory variables. Redundant variables have already been identified by the variance inflation factor and removed from the analysis. The residuals were normally distributed. Finally, the OLS model was controlled for spatial autocorrelation of the regression residuals. The Moran's I statistic (Mitchell, 2005) showed that the residuals were random, and that there was no significant clustering on the residuals (Moran's Index = 0.03, p = 0.4, Z = 0.82). Furthermore, the Hotspot analysis using the Getis-Ord Gi* statistic confirmed that there was no significant over- or under- prediction (Residuals were randomly distributed; not clustered) (Fig. 5)

Table 4. Summary of OLS Results in components 1 and 2.

Component 1 (Band 7 and Tasseled cap 3)								
Variable	Coefficient	Std	t-Statistic	Probability	Robust_SE	Robust_t	Robust_Pr	VIF
Intercept	-14.549	1.546	-9.409	0.00000*	1.633	-8.908	0.00000*	------
Band7	0.476282	0.0384	12.411	0.00000*	0.04432	10.7466	0.00000*	6.025
Tas. Cap3	0.392781	0.0646	6.075	0.00000*	0.0685	5.7328	0.00514*	6.025
Component 2 (Band 1 and PCA2)								
Variable	Coefficient	Std	t-Statistic	Probability	Robust_SE	Robust_t	Robust_Pr	VIF
Intercept	-31.6604	4.305	-7.353	0.0000*	4.1060	-7.7107	0.0000*	------
Band1	0.3761	0.0370	10.161	0.0000*	0.0358	10.502	0.0000*	6.173
PCA2	0.1469	0.0486	3.0204	0.0028*	0.0520	2.8246	0.0051*	6.173

OLS Diagnostics in components 1 and 2

Adjusted R-Squared [2]:	0.575601	Adjusted R-Squared [2]:	0.594706
Akaike's Information Criterion (AIC) [2]:1416.651140		Akaike's Information Criterion (AIC) [2]:1405.78045	
Joint F-Statistic [3]:	160.361928	Joint F-Statistic [3]:	173.413078
Joint Wald Statistic [4]:	321.779504	Joint Wald Statistic [4]:	331.959979
Koenker (BP) Statistic [5]:	17.113055	Koenker (BP) Statistic [5]:	18.025068
Jarque-Bera Statistic [6]:	3.485322	Jarque-Bera Statistic [6]:	3.972697

Notes on Interpretation

* Statistically significant at the 0.05 level.

[1] Large VIF (> 7.5, for example) indicates explanatory variable redundancy.

[2] Measure of model fit/performance.

[3] Significant p-value indicates overall model significance.

[4] Significant p-value indicates robust overall model significance.

[5] Significant p-value indicates biased standard errors; use robust estimates.

[6] Significant p-value indicates residuals deviate from a normal distribution.

Figure 5. Residual map (Blue point shows under-prediction and Red point shows over-prediction).

Validation

In order to evaluate the model performance a cross-validation method in Eyvanekey Plain was applied. Eyvanekey plain consists of similar environmental characteristics, compared to the study area in this research. All 52 sample points were employed for model validation. Two resulted models were tested for 52 soil samples. MAE (Mean Absolute Error) and RMSE (Root Mean Square Error) are compared in Table 6. Model-2 (B1-PCA2) performs better than Model-1 (B7-Tasseled 3) (Table 5).

Table 5. Cross validation

	Mode1(B7-TASSEL3)	Model 2(B1-PCA2)
MAE	0.58	0.49
RMSE	4.43	4.10

To analyze the sensitivity of the predicted parameters in these models, a sensitivity analysis was performed by sensitivity index approach.

Sensitivity of Predicted Parameters to Soil EC

The parameters that were tested in the sensitivity analysis for predicted soil EC were Band-1 and Band-7, PCA2 and Tasseled cap3. Of the two parameters/variables that were tested for sensitivity in soil EC prediction, Band-7 and Band-1 came out as the most sensitive parameters, based on the sensitivity index (eq1). Band-1 proved to be more than three times more sensitive than PCA2 in the model 2, and Band-7 more than two times more compared to Tasseled cap3 (Figs. 6 and 7). Thus, efforts and resources

should be spent on quantifying these parameters for an accurate and reliable salinity prediction.

The magnitude of output variations is the result of the variation in model input parameters. When a selected parameter is given a higher or lower value by a certain percentage and the other parameters are kept constant, the output values varied by the same percentage. The range of parameter variations was determined primarily in preliminary runs according to the sensitivities of selected parameters. The Lane and Ferreira criterion (1980) was applied to define whether or not a tested parameter or input variable was sensitive; a model parameter or input variable is defined as sensitive if errors in that parameter or input variable cause errors in output variables as large as or larger than the input parameter errors. The sensitivity index (Si) for a parameter or

variable was defined as:

$Si=(Pi-Pib)/(Pib)*100$

Where: *Pi* is the prediction with varying parameter/variable i, and *Pib* is the same prediction with the corresponding base value.

This sensitivity index is different from the commonly used sensitivity coefficient, which is a partial derivative representing the change in model outputs resulting from a change in a model input. The problem with the usual sensitivity coefficient is that the magnitude of sensitivity depends on both the dimension and units of parameters. One may calculate sensitivities for two parameters that are numerically equal; however, they may not be dimensionally identical. Thus, simply comparing numerical values (sensitivity coefficients) calculated according to the derivative may be inadequate (Tables 6 and 7).

Table 6. Sensitivities of parameter variation in model 1.

	Parameters				
Model 1				**Change in prediction**	**Sensitivity Index**
		Tasseled 3	**Band-7**	**Predicted EC**	
Base run	0	-49	113	19.98		
Variation (% of base value) band 7	+20	constant	135.6	30.74	0.5384	2.692
	-20	constant	90.4	9.22	-0.5384	-2.692
Variation (% of base value) Tasseled 3	+20	-39.2	constant	23.83	0.193	0.963
	-20	-58.8	constant	16.13	-0.193	-0.963

Table 7. Sensitivities of parameter variation in model 2.

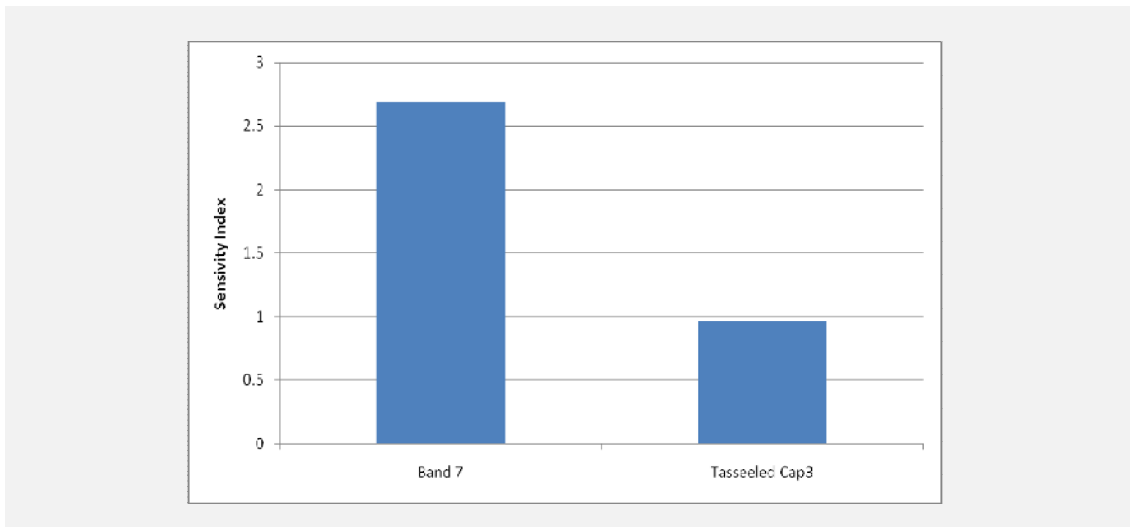| **Model 2**				**Change in prediction**	**Sensitivity Index**
		PCA2	**Band-1**	**Predicted EC**	
Base run	0	-10	131	16.126		
Variation (% of base value) band 1	+20	constant	157.2	25.9772	0.6109	3.054446
	-20	constant	104.8	6.2748	-0.6109	-3.05445
Variation (% of base value) PCA2	+20	-8	constant	16.42	0.0182	0.091157
	-20	-12	constant	15.832	-0.0182	-0.09116

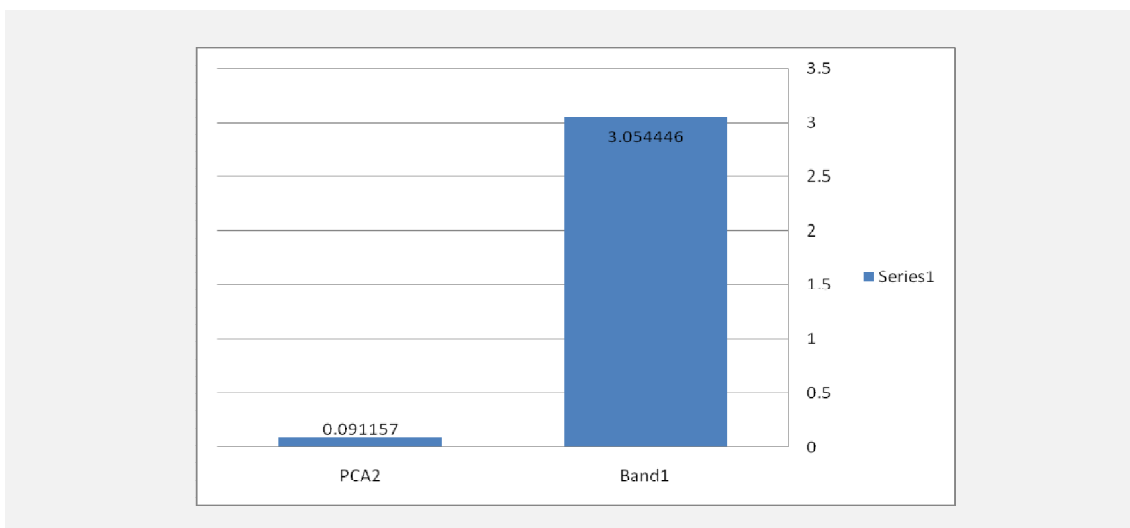**Figure 6.** Sensitivity index for parameters in model-1.

Figure7. Sensitivity index parameter model 2.

Conclusions and Recommendations

The mapping and monitoring of soil salinity is required for sound agricultural planning to ensure food security. However, the process of mapping salt-affected areas is often difficult as salt may exist in many forms even in the case of those visually appearing on surface. This becomes even more difficult in soils with salt concentrated in the substratum, which may eventually move to the soil surface due to capillary rise.

EC measurement is customary practice for defining and assessing soil salinity (Homaee and Schmidhalter, 2008). Spectral information that can be extracted from remote sensing data is a useful indicator of EC. Among others, mid-

infrared band (Landsat band-7) and visible band (band-1) are strongly associated with the observed EC. Among derived bands, Tasseled cap 3 and PCA2, which have a very high association with EC, are significant predictors of EC.

Developed salinity prediction models, particularly the ones containing spectral variables, can be useful to infer soil salinity over large areas using remote sensing data. Considering that the soil and remote sensing data that were used in this study represent only one image of the area in the year, i.e. the middle period of the dry season, the use of multi-temporal soil and remote sensing data within a year and over a number of years must be recommended for monitoring purposes.

References

Abbassi, H. (2009). Monitoring of soil and water characteristic in Garmsar Plain. Research Institute of Forests and Rengelands. 82-0320417000-07.

Alavi Panah, S.K. and G.H. Zehtabian (2002). A data base approach for soil salinity mapping and generalization form Remotely Sensed data and geographic information system. FIGXXI. International Congress, Washington, D.C. USA.

Andri Baltensweiler, S.Z. (2010). Modeling soil Acidity in Switzerland using spatial statistics tools. Proceedings of the ESRI International User Conference, July 12-16, 2010 (1493).

Clifford, P., S.Richardson and D. Hemon (1989). Assessing the significance the correlation between two spatial processes. *Biometrics* 45: 123-134.

Darvishsefat, M., A.A. Damavandi, M. Jafari and G.H. Zehtabian (1999). Study on feasibility salt affected soil classification by Landsat Imagery. *Journal of Deserts* 5(2).

Draper, N. and H. Smith (1998). Applied Regression Analysis, 3rd ed. New York: Wiley.

Dwivedi, R., K.V. Ramana, S.S. Thammappa, A.N. Singh (2001). The utility of IRS-1C LISS-III and PAN-merged data for mapping salt-affected soils. *Photogrammetric Engineering and Remote Sensing*, 67: 1167–1175.

Dwivedi, R.S. and K. Sreenivas (1997). Delineation of salt-affected soils and waterlogged areas in the Indo-Gangetic plains using IRS-1c LISS-III data. *International Journal of Remote Sensing*, 19.

Epstein, E., J.D. Norlyn, D.W. Rush, R.W. Kingsbury, D.B. Kelly, G.A. Cunningham and A.F. Wrona (1980). Saline culture of crops: A genetic approach. *Science*, 210:399.

FAO. (2008). The State of Food Insecurity in the World 2008. Food and Agriculture Organization of the United Nations., Rome, Italy ISBN 978-92-5-106049-0.

Farshad, A. (2008). Lecture notes on Salinization/Alkalinization; Monitoring and Evaluation. ITC publication.

Fotheringham, A.S., C. Brunsdon and M. Charlton (2002). Geographically Weighted Regression: The Analysis of Spatially Varying Relationships. Chichester: Wiley & Sons.

Ghabour, T.K. and L. Daels (1993). Mapping and Monitoring of soil salinity of ISSN. *Egyptian Journal of Soil Science*, 33(4): 355-370.

Hair, J.F., A.R. Tatham, R.L., W.C. Black (1992). Multivariate Data Analysis with Readings. New York: Macmillan Publishing Company.

Hastie, T., R. Tibshirani and J. Friedman (2001). The elements of statistical learning: Data mining, inference, and prediction. New York: Springer.

Homaee. M. and U.R.S. Schmidhalter (2008). Water integration by plants root under non-uniform soil salinity. *Irrigation Science*, 27: 83-95.

Howari, F. (2003). The use of remote sensing data to extract information from agricultural land with emphasis on soil salinity. *Australian Journal of Soil Research*, 41: 1243.

Lane. L,J. and V.A. Ferreira (1980). Sensitivity analysis, in CREAMS-a field scale model for chemical, runoff, erosion from agricultural management systems. In Knisel, W.G. (Ed.) USDA Conservation Recourse Report 26 (USDA, Washington, DC,): 113–158.

Madrigal L.P., W.C., J.G Meraz, Rubio BDR, Ramı́rez OL (2003). Soil salinity and its effect on crop yield: A study using satellite imagery in three irrigation districts. *Ingenieria Hidraulica en Mexico*, 18: 83–97.

Menenti, M., A. Lorkeers, M. Vissers (1986). An application of Thematic Mapper data in Tunisia. *ITC Journal*, 1: 35–42.

Metternicht, G. and J.A. Zinck (2003). Remote sensing of soil salinity: Potentials and constraints. *Remote Sensing of Environment*, 85: 1-20.

Metternicht, G. and J.A. Zink (2009). Remote Sensing of Soil Salinization Impact on Land Management. CRC Press, Taylor & Francis Group.

Mitchell, A. (2005). The ESRI guide to GIS analysis. Spatial Measurements and Statistics. ESRI Press Redlands (CA). 2.

Momeni, A. (2007). Land Unit and Land resources map Preparation in one million Scale. Soil and Water Research Institute Report.

Naseri, M.Y. (1998). Characterization of salt-affected soils for modeling sustainable land management in semi-arid environment: A case study in the Gorgan region, Northeast Iran. PhD Thesis, Ghent University: 321p.

Pakparvar, M. (2004). Monitoring of soil and water characteristics in Garmsar Plain. Research Institute of Forests and Rengelands. 75-0310417136-3.

Richards, L. (1954). Diagnosis and Improvement of Saline and Alkali Soils. Agriculture Handbook US Department of Agriculture, Washington, DC(60).

Saha,S.K., K.M., S.K. Bhan (1990). Digital processing of Landsat TM data for wasteland mapping in parts of Aligarh District, Uttar Pradesh, India. *International Journal of Remote Sensing*, 11: 485–492.

Shresta. D. and A. Farshad (2009). Mapping salinity Hazard: An integrated application of remote sensing and modeling-based techniques. Chapter12 in Remote Sensing of Soil Salinization Impact on Land Management. CRC Press, Taylor & Francis Group.

USSLS. (1969). Diagnosis and Improvement of Saline and Alkali Soils. Agriculture Handbook United States Salinity Laboratory Staff, US Government Printing Office: Washington, DC 60.

Verma, K.S., S.R., A.K. Barthwal, S.N. Deshmukh (1994). Remote sensing technique for mapping salt affected soils. *International Journal of Remote Sensing*, 15: 1901–1914.